Strong to weak coupling transition in low misorientation angle thin film $YBa_2Cu_3O_{7-x}$ bicrystals

N. F. Heinig, R. D. Redwing, J. E. Nordman, and D. C. Larbalestier
Applied Superconductivity Center, University of Wisconsin, Madison, Wisconsin 53706
(Received 10 November 1997; revised manuscript received 9 February 1999)

Detailed transport measurements were made of $YBa_2Cu_3O_{7-x}$ thin-film [001] tilt bicrystals with misorientation angles of 3°, 5°, 7°, 10°, 15°, and 20°, encompassing the angular regime where the transition from strong to weak coupling occurs. The study includes measurements of intragrain and intergrain extended voltage-current characteristics in applied magnetic fields that range from zero to well above the irreversibility field. The results show that the strong-to-weak coupling transition is progressive at 77 K, occurring at misorientation angles between 7° and 10° in zero field, and between 10° and 15° in higher magnetic fields. The shapes of the voltage-current characteristics of the 7° [001] bicrystals and the ratio of the inter- and intragranular critical current densities are particularly sensitive to individual sample preparation conditions, suggesting that substrate-film interdiffusion along the grain-boundary dislocations is controlling the effective size of the superconducting channels between the dislocation cores. The linear decline of the intergranular critical current density with misorientation angle predicted from present dislocation core overlap models is not found, showing that additional features of the grain-boundary nanostructure and the mechanism of intergranular current flow need to be invoked in order to explain transport across low-angle $YBa_2Cu_3O_{7-x}$ grain boundaries.
[S0163-1829(99)02626-0]

I. INTRODUCTION

Among the largest obstacles to bulk-scale, high power applications of high-temperature superconductors (HTSC's) are the low critical current densities and weak superconducting coupling across grain boundaries (GB's) of arbitrary misorientation angles. Most large scale applications demand large critical currents in magnetic fields of a Tesla or more, requiring that a significant fraction of the conductor consists of a strongly coupled superconductor. It is well established that the intergranular critical current density J_b, in [001] tilt thin-film bicrystals of high-temperature superconductors, is very dependent on the misorientation angle, θ, of the GB.[1–5] As θ increases from 0° to 25°, J_b decreases and the intergranular coupling changes from strong and single crystal-like, to weak and Josephson junctionlike. Experiments on different types of $YBa_2Cu_3O_{7-x}$ samples have reported that the crossover from strong to weak coupling can vary over a wide angular range of 5° to 20°,[1,4,6–8] although the criteria for deciding when the transition occurs are not always explicit or consistent.

A good understanding of low-angle grain boundary transport is both intrinsically interesting and very relevant to the recently developed $YBa_2Cu_3O_{7-x}$ coated conductors. These quasisingle crystalline, biaxially textured, thick films can have very high J_c values. They also have excellent potential to be made in long lengths, making them useful for high current applications. With a buffer/substrate layer between the nickel alloy and the superconductor, and using ion-beam-assisted deposition to encourage grain alignment of the Y_2O_3-stabilized ZrO_2 substrate layer, $J_c(77\,\mathrm{K})$ values of order $1\times10^6\,\mathrm{A/cm^2}$ in 1–2 μm thick layers have been achieved.[9–12] Another technique, rolling-assisted biaxially textured substrates,[13] produces high-J_c material by using a textured Ni substrate with one or more intermediate buffer layers between the substrate and the $YBa_2Cu_3O_{7-x}$ layer. This technique now yields very comparable $J_c(77\,\mathrm{K})$ values. While these are encouragingly high critical current densities, magneto-optic imaging studies[14] show that J_c is still limited by percolation in these textured polycrystalline samples. Understanding the current flow through the array of low-angle grain boundaries and other barriers that form in these materials is essential to raising J_c and advancing this technology. Understanding the current flow across individual low-angle grain boundaries, over the range of field and temperature that such conductors are likely to be used, is an important first step to accomplishing these goals.

The simple model which is most widely used to explain this transition from strong to weak coupling postulates that the strongly coupled supercurrent across the grain boundary is restricted to channels between the grain-boundary dislocation cores or their strain fields.[1,15] Since the dislocation spacing becomes smaller with increasing angle θ, it is natural to postulate that no strongly coupled superconducting path across the boundary should exist above some critical misorientation angle θ_c. This model provides a conceptually reasonable explanation of why grain boundaries of increasing misorientation angle undergo a transition from strong to weak coupling with increasing θ. However, neither the effective size of the grain-boundary dislocations, nor the details of the grain-boundary dislocation networks are usually known, thus leaving the channel width and transition angle quite uncertain. There is also increasing evidence that low-angle grain boundaries have quite heterogeneous dislocation structures. The dislocations can have multiple Burger's vectors, be partial or primary in nature and be spaced nonuniformly.[16–18] In addition, the grain boundary can be faceted and have compositional variations associated with the facets. Such heterogeneous GB's may well support parallel resistive, Josephson coupled, and strongly coupled current paths, complicating any interpretation of the measured current-voltage characteristics.[19] Thus, whatever the concep-

tual reasonableness of the channel model, it needs more quantitative verification, both to understand how the supercurrent passes through constricted channels, and because this is an important technological issue for coated conductors, where some spread in the grain-to-grain alignment is inevitable.

Another check of the dislocation core model can be found by comparing bulk scale and thin-film transport data. While the dislocations that form thin-film and bulk scale grain boundaries should be similar, there is poor agreement between the results on bulk and thin-film bicrystals of $YBa_2Cu_3O_{7-x}$. For example, flux grown, bulk scale [001] tilt bicrystals with θ less than 10° tend to be strongly coupled,[20] while the electron beam evaporated thin-film bicrystals of Dimos *et al.*[1] showed weak-coupling behavior at angles as low as $\theta=5°$. Irreversibility field measurements by Cai *et al.*[21] suggest that strongly coupled channels can exist across 15°, 18°, and 27° [001] tilt bulk scale bicrystals. Parikh *et al.*[22] and Field *et al.*[6] have provided evidence for strongly coupled components in GB's of mixed misorientation angles exceeding 10° in melt-textured bulk scale $YBa_2Cu_3O_{7-x}$. Thus there is considerable variation in the properties of different $YBa_2Cu_3O_{7-x}$ grain boundaries and no general agreement on the misorientation at which boundaries become completely weakly coupled. This uncertainty is compounded by the fact that most work has only reported the ratio of the intergranular and intragranular (J_b/J_c) current densities, evaluated in zero applied field. Very little high magnetic-field data is available, and there are even fewer details about the extended electric field-current density (E-J) characteristics of individual grain boundaries.[23]

This paper describes the extended transport behavior in both low and high fields of [001] tilt $YBa_2Cu_3O_{7-x}$ bicrystal thin films with misorientation angles between 3° and 20°, comparing the results to what would be expected from dislocation overlap models. Section II of the paper describes the experimental details, Sec. III the zero-field transport behavior, while Sec. IV shows how the voltage-current characteristics change with misorientation angle in high magnetic fields, and uses this information to compare the inter- and intragranular irreversibility fields, H^*. The variations in properties of several bicrystals with $\theta=7°$ are also presented and discussed. Section V discusses and summarizes the results.

II. EXPERIMENTAL DETAILS

The $YBa_2Cu_3O_{7-x}$ thin-film bicrystals with thicknesses ranging from 0.10 to 0.25 μm were grown on 0.5×1 cm [001] $SrTiO_3$ bicrystal substrates made by the Shinkosha Co. using pulsed-laser ablation (PLD) in a KrF laser system operated at 5 Hz and a wavelength of 248 nm. The $YBa_2Cu_3O_{7-x}$ was grown in an oxygen atmosphere of 200 mTorr on substrates kept at 730–760 °C. The temperature was extrapolated from optical pyrometer measurements of a point on the substrate-mounting block outside of the $YBa_2Cu_3O_{7-x}$ plume. After growth, the films were processed to make well-defined test links: a single intragranular link and a number of intergranular links of varying width were made. Gold contact pads were sputtered onto the films by using a shadow mask and the links were defined using photolithography and ion-beam milling. The voltage tap traces were 500 μm apart for the intragrain link and 100 μm apart for the intergrain links.

Considerable care was taken to obtain extended E-J curves over a wide range of electric and magnetic field. The gold pads on the sample were contacted with spring-loaded, gold-plated pins connected to a Keithley Instruments 1801 nanovolt preamplifier. Current was fed to the films with a Keithley Instruments 224 precision current source and a current reversal algorithm was used to minimize systematic thermoelectric voltage error. The zero field critical current density measurements were done inside a μ metal shield placed in a screened room in order to reduce the earth's magnetic field and rf noise.

The high-field measurements were made in a 14 T superconducting magnet with the applied field perpendicular to the film surface and thus to the c axis of the $YBa_2Cu_3O_{7-x}$. Most of the data were taken in a He-gas-cooled variable temperature insert. Some of the higher angle bicrystals were also measured in a more stable 1 T Cu magnet, whose field fluctuations were ±0.04 mT. This greater stability reduced the voltage noise due to Josephson vortex motion that was seen in the measurements made on weak-linked samples in the noisier superconducting magnet. Both intragrain and intergrain voltage-current characteristics were measured for each value of the magnetic field for each bicrystal. For higher angle bicrystals, wider intergranular links were chosen for the high-field measurements, so that comparable inter and intragrain critical currents were measured.

III. ZERO-FIELD BEHAVIOR

Figure 1 shows the ratio of inter- and intragranular critical current densities, J_b/J_c, versus θ for the PLD thin-film bicrystals measured at 77 K and zero applied field using data taken from the 5 and 10 μm wide links, so as to provide the best comparison to the 10 μm wide intragranular link. Each misorientation angle; 3°, 5°, 7°, 10°, 15°, 20°, and 24°, is represented by data from between one and four different bicrystal samples, so as to show scatter due to variations between growth runs. Our PLD data set is indicated by the circles in Fig. 1, where it is also compared to the original electron-beam-evaporated (EBE) $YBa_2Cu_3O_{7-x}$ [001] tilt bicrystal data (squares) taken from Dimos *et al.*[1] The EBE bicrystals were measured in zero applied field at 5 K, and the J_b/J_c ratios are calculated from the J_b and J_c values given in Ref. 1.

On the whole, the EBE films have a qualitatively similar J_b/J_c versus θ relationship as our PLD grown films, but possess generally lower J_b/J_c ratios. This occurs even though the EBE data were taken at 5 K, rather than at 77 K. The greater number of data points for our PLD samples show that the ratio of J_b/J_c can be almost as high as unity for θ between 0° and 7°. However, the exponential behavior at higher angles fits well with that observed by Ivanov *et al.*[4] for bicrystals grown by PLD on yttria-stabilized zirconia substrates. This exponential decrease between 7° and 36° can be seen in the inset to Fig. 1, where the absolute values of J_b are plotted.

Plotted as dashed lines in Fig. 1 are the predictions of the channel model for values of $r_m=0.39$ and 1.13 nm, corre-

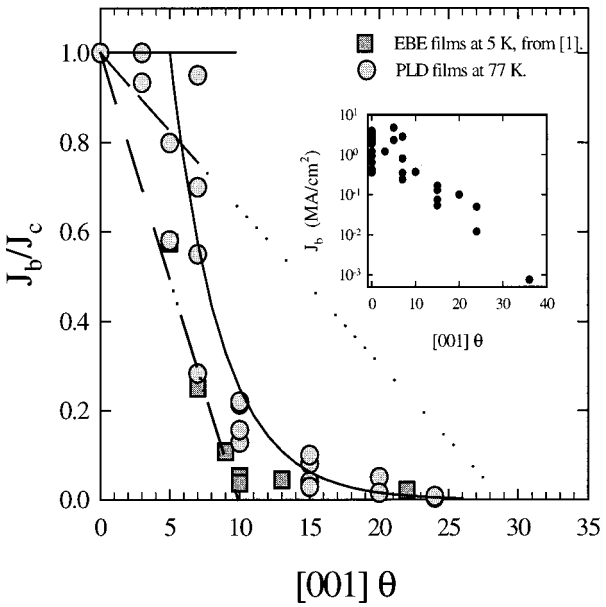

FIG. 1. Normalized $J_b/J_c(0T)$ ratio versus $[001]\theta$ using electron-beam-deposited thin-film data from Dimos *et al.* (Ref. 1), taken at 5 K, and pulsed-laser-ablated thin films from this work, taken at 77 K. The solid lines show two distinct trends, one of an approximately constant J_b/J_c up to 7°, and the second an exponential decrease starting at higher angles. The dashed lines show the predictions of the simple dislocation core overlap model for $r_m=|\mathbf{b}|$, and $r_m=2.9|\mathbf{b}|$. The inset shows the PLD film data on a semilogarithmic plot without normalization.

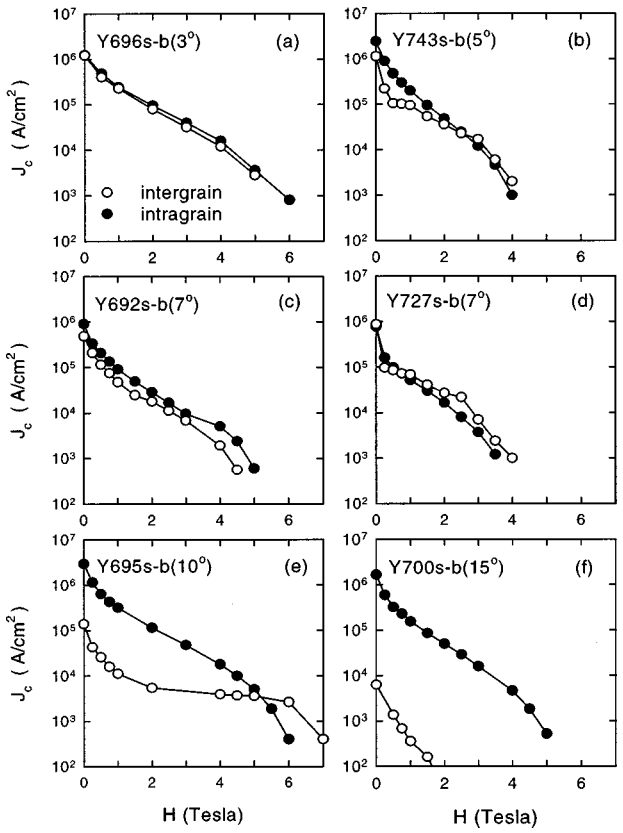

FIG. 2. J_c versus H at 77 K, $H\|c$, with J_c defined by a 1 μV/cm criterion. Both intergrain and intragrain J were measured for each bicrystal film: (a) 3°, (b) 5°, (c) 7°, (d) 7°, (e) 10°, (f) 15°. Intergrain properties are indicated by open circles and intragrain by closed ones.

sponding to the estimated range of the effective core size (1 to 2.9 b) in the literature.[1,15] The change from long to short dashes indicates when the channels between the dislocation cores become less than a coherence length wide. Since the coherence length decreases with decreasing temperature, the ratio of J_b/J_c should be larger at 5 K than at 77 K, and the critical crossover angle from strong to weak coupling, θ_c, should also be larger. However, when comparing the EBE data with our PLD data, the opposite effect is suggested. In contrast to high-angle grain-boundary transport behavior, where there is good agreement between different studies, the lower angle data of this study suggest that low-angle grain-boundary transport behavior is significantly affected by the growth process.

The PLD bicrystal data clearly show two distinct regimes of behavior, one at low angles ($\theta<\sim7°$) where there is essentially no depression of J_b for the better films, and one at higher angles, where J_b exponentially declines with increasing θ. This dual behavior is shown explicitly in Fig. 1 by the two solid lines. The goal of further understanding the strongly coupled bicrystals ($\theta<\sim7°$), and the differences between bicrystals with the same misorientation angle led to more detailed current-voltage measurements in high magnetic fields.

IV. HIGH MAGNETIC-FIELD BEHAVIOR

Figure 2 shows the intra- and intergrain $J_c(H,77\,\mathrm{K})$ curves for the magnetic field parallel to the c axis at the standard criterion of 1 μV/cm for a number of low-angle bicrystals. All the intragranular data show an approximately exponential decrease in J_c with magnetic field, which can be expressed as $J_c=J_{c0}e^{-\alpha H}$, where J_{c0} is the zero-field J_c, H is the applied magnetic field, and α is the rate of decrease. This rate of decrease varies from 1.2 to 2 T^{-1} for the data in Fig. 2, although some films had α as high as 3 T^{-1}. This field dependence is common for intragranular behavior of $YBa_2Cu_3O_{7-x}$ films. In contrast, the intergranular $J_c(H)$ data show significant deviations from exponential behavior.

The intergranular $J_c(H)$ characteristics of Fig. 2 show a variety of behavior. For the 3° and one 7° [001] tilt bicrystal [Figs. 2(a) and 2(c)], the intergrain $J_c(H)$ curves also behave exponentially and are almost indistinguishable from the intragrain curves. The other bicrystals show an intergrain $J_c(H)$ that decreases more rapidly than the corresponding intragrain curve in lower fields, then flattens out and decreases more slowly than the corresponding intragranular curve. This is most obvious for the 10° bicrystal in Fig. 2(e), but can also be seen in the 5° [Fig. 2(b)], and a second 7° [Fig. 2(d)] bicrystal. In Fig. 2(d), this 7° bicrystal appears to have a zero-field intragrain J_c which is less than the intergrain value; however, this is an artifact due to damage sustained by the intragrain link during thermal cycling. Finally, for the higher angle 15° and 20° bicrystals, a rapidly decreasing $J_c(H)$ is seen for all fields, with no evidence of any convergence of the inter and intragrain $J_c(H)$ at higher magnetic fields.

The data sets show that the grain boundary $J_c(H)$ decreases more rapidly than that of the intergranular link in

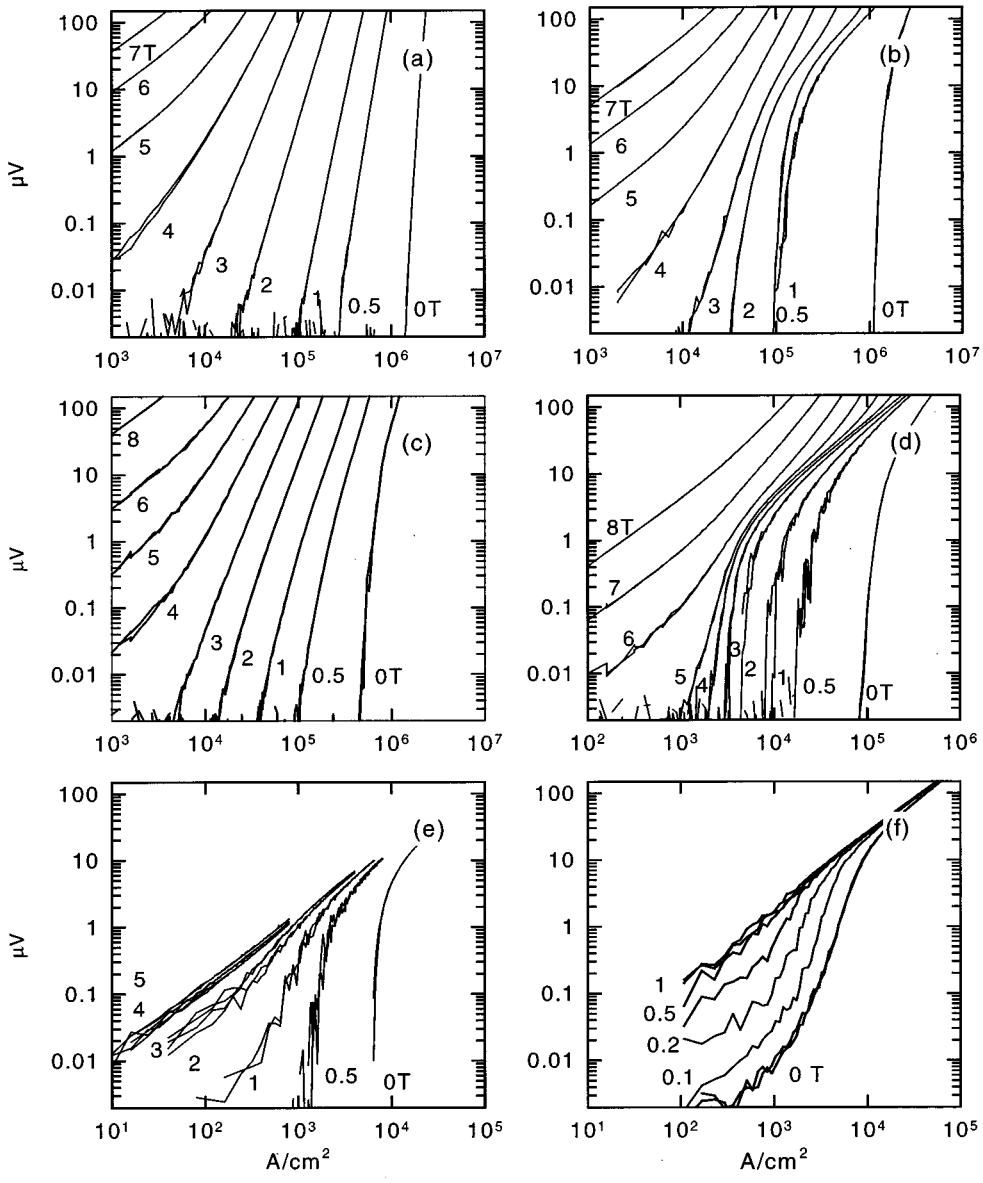

FIG. 3. Voltage-current density characteristics at 77 K, in applied magnetic fields with $H \| c$. The intergranular characteristics for (a) 0°, (b) 5°, (c) 7°, (d) 10°, (e) 15°, and (f) 20° $YBa_2Cu_3O_{7-x}$ grain boundaries.

lower fields and that the two characteristics tend to converge at higher fields. It is also to be noted that the changes in intergranular $J_c(H)$ properties are gradual, rather than sudden. However, because the intergranular electric field becomes progressively more localized at the grain boundary as θ increases, it is also important to compare the extended voltage–current density (V-J) curves. We prefer to plot the V-J, rather than the electric field–current density (E-J) characteristic because of this localization of E at the boundary. Nominal electric-field values may be obtained by dividing the voltages by the tap lengths of the intragranular (500 μm) and the intergranular (100 μm) sections.

Further reasons for measuring extended V-J characteristics are that they clearly show the growth of resistance at the boundary with increasing θ and because they permit us to develop a more rigorous criterion for channel closure than that given by the ratio of J_b/J_c at zero field. As already discussed,[23] one such criterion is the existence of *intergrain* voltage-current density (V-J) characteristics that exhibit qualitatively similar properties to the *intragrain* characteristics. The basis of this criterion is the search for evidence of the irreversibility field H^* in both the intragrain and the intergranular V-J characteristics. So long as this can be observed in both sets of characteristics, we assert that strongly coupled channels are open across the grain boundary. One merit of this criterion is that intragranular high-field properties of single-crystal $YBa_2Cu_3O_{7-\delta}$ films are well known,[24] leading to a minimum of ambiguity.

Figure 3 collects some of these V-J curves at various magnetic fields plotted on a double logarithmic scale. These data correspond to the 5°, Y692s-b(7°), 10°, and 15° bicrystals, which are also featured in Fig. 2. In addition, the V-J curves of Y747s-b(20°), measured in the 1 T Cu magnet, can be seen in Fig. 3(f). As in the $J_c(H)$ curves, a clear progression in their shape with increasing grain-boundary misorientation angle is seen.

In Fig. 3(a), the extended V-J curves of a typical intragranular link at different magnetic fields are plotted. The curves are smooth and almost linear on the double logarithmic scale, with a slight downward curvature in low fields and a slight upward curvature at higher fields. The field at which this curvature changes sign, corresponding to the irreversibility field, H^*, is about 3 T, which is close to the value of 4 T derived by Koch *et al.*[24] from their measurements of the field-dependent vortex-glass transition temperature in single-crystal thin-film $YBa_2Cu_3O_{7-x}$. The transition at H^* corresponds to the crossover from flux-pinning-dominated behavior below H^* to a flux-flow state at fields above H^*.

Both the 3° (not shown) and the Y692s-b(7°) bicrystal [Fig. 3(c)] intergranular V-J curves appear very similar to the intragranular curves of Fig. 3(a), showing that it is possible to have a significant GB misorientation angle before the boundary seriously obstructs supercurrent flow. However, it is also clear that the V-J curves do show more structure, particularly at higher voltages, as the misorientation angle increases. Figure 3(b) shows the intergranular V-J curves for a 5° bicrystal. Consistent with the $J_c(H)$ data in Fig. 2(b), the V-J curves are quite far apart between 0 and 0.5 T, are quite closely spaced between 0.5 and 4 T, and then resemble the intragranular V-J curves above 4 T. As a whole, the curves show the continuous growth of dissipation at the GB, which tends to becomes more and more Ohmic as θ increases, compatible with the appearance of more resistive components in the grain boundary. This is consistent with preferential flux flow across the dislocation cores lying in the boundary. Above H^* there is an increasing contribution to the total dissipation of the *intergranular* link from the *intragranular* portions of the link. However, by 15° and 20°, the dissipation at the boundary is so large that any additional dissipation from the banks is negligible.

An additional sign of the weak coupling at the boundary is the appearance of extra voltage noise in the V-J characteristic, which can attain several microvolts, and which gradually decreases as the magnetic field increases. Because our superconducting magnet did not operate in persistent mode, we expect that this noise was generated by small fluctuations of the magnetic field that cause flux hopping in the weakly pinned, Josephson-coupled segments of the grain boundary.

To determine the irreversibility field H^*, a phenomenological approach was used.[25,26] On a double-logarithmic scale, H^* occurs when the voltage-current V-I characteristic changes curvature. If the V-I characteristic is then fit to a quadratic:

$$\ln(V) = a + b\ln(I) + c(\ln(I))^2, \tag{1}$$

where a, b, and c are fit parameters, H^* is defined when $c = 0$, which corresponds to a straight line on a double logarithmic scale. This method finds H^* as the field where the V-I curve most closely resembles a power law.

Because of the tendency of the V-J curves of higher angle bicrystals to exhibit a crossover to linear behavior at high voltages, the whole intergranular V-J characteristic at any given field will obviously not fit Eq. (1). Accordingly, our fit is restricted to the low-voltage regions of the V-J curve, and we justify this by noting that there are two kinds of transport behavior across the grain boundary. At low voltage levels, the transport is characterized by the power-law-like properties of the grains and any strongly coupled paths across the GB, while at higher voltages, flux flows preferentially along the boundary, giving rise to an increasingly Ohmic V-I characteristic. Since the strongly coupled channels across the GB are the feature of interest for the determination of θ_c, only the low voltage region was fit to Eq. (1). At sufficiently high magnetic fields and voltages, the intragrain regions on either side of the GB also become dissipative, causing the V-I characteristic to change back from linear to power law.

TABLE I. Irreversibility fields at 77 K.

Sample	H^*_{GE} (T)	H^*_{Grain} (T)
Y696s-b(3°)	3.0	3.5
Y743s-b(5°)	3.5	2.6
Y692s-b(7°)	3.5	4.0
Y695s-b(10°)	5.5	3.8
Y700s-b(15°)	0.7	3.8
Y747s-b(20°)	0	

Both intragrain and intergrain V-I curves were fit to Eq. (1), using the magnetic field at which the c parameter goes to zero to define H^*. The results of this analysis are summarized in Table I, which shows the inter- and intragrain H^* for each sample within an error bar of approximately ± 0.5 T.

For misorientation angles at or below 10°, the inter- and intragranular $H^*(77\,\mathrm{K})$ values were rather similar. Between 10° and 15°, $H^*_{GB}(77\,\mathrm{K})$ dropped sharply, becoming much less than that of the intragranular region, and by 20° no downward curvature of the double-logarithmic V-I characteristic was seen, even at zero field. Focusing on the data set of Table I, we see that the H^* values derived from measurements of the intragranular curves ranged from 2.6–4.0 T, while the intergranular H^* values ranged from 3.0 to 3.5 T (3°–7°), was 5.5 T at 10°, fell sharply to 0.7 T (15°), and then became 0 T at 20°. We do not understand the strong enhancement of H^* at 10°, which may be a limitation of our evaluation procedure in the limit of almost closed channels.[27] Since H^* is measured from the low-voltage regions of the V-I curve that are dominated by transport through the strongly coupled GB segments, the strong depression of H^*_{GB} in the 15° bicrystal indicates that strongly coupled channels no longer exist, signaling that the transition misorientation angle between strong and weak coupling occurs between 10° and 15° for these laser-ablated films.

The variation in high-field transport properties for a single misorientation angle can be seen explicitly in Fig. 4, which shows the intergranular V-J curves of three different 7° [001] tilt bicrystals. In Fig. 4(a), the intergranular curves are close to power law, similar to those of a single crystal. In Figs. 4(b) and 4(c), there appears to be a significant weakly coupled component to the V-J characteristic. In sample Y752s-b(7°), seen in Fig. 4(c), the intergrain J_c drops off very rapidly in field, corresponding to the low intragrain H^* values seen in this particular film. These bicrystals were grown several months apart, and several modifications to the

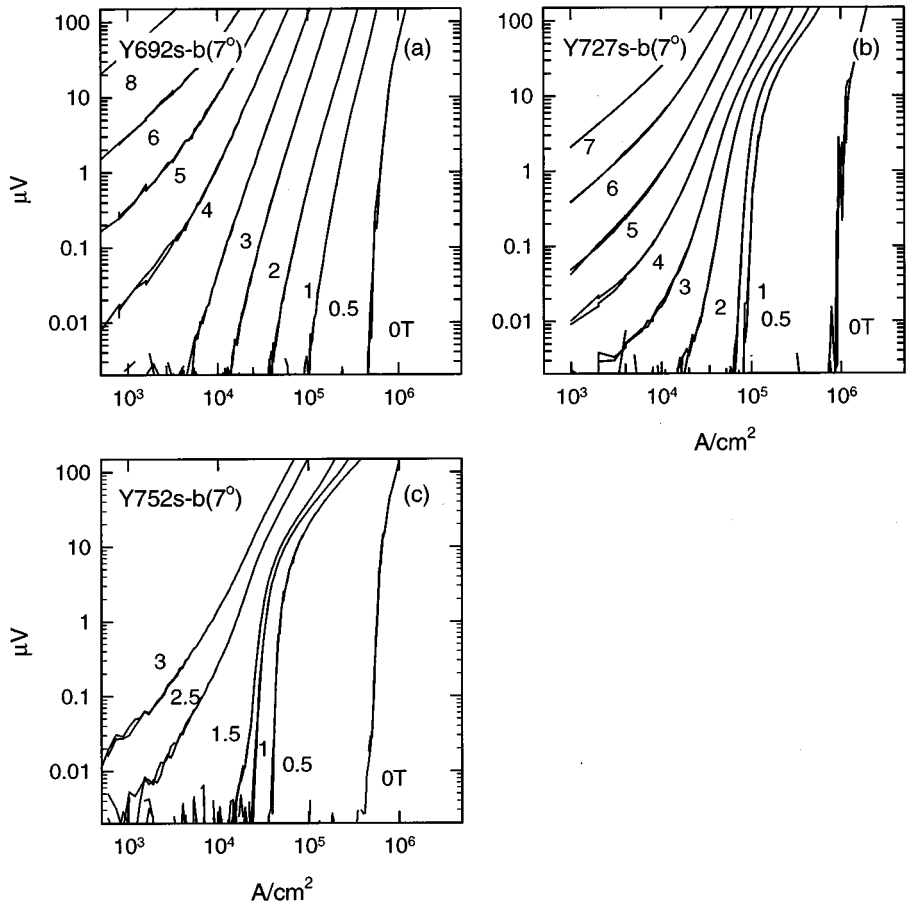

FIG. 4. Intergranular V-J curves for $H \| c$ in large magnetic fields at 77 K for (a) Y692s-b(7°), (b) Y727s-b(7°), and (c) Y752s-b(7°).

growth chamber were made in the interim, making it difficult to determine which variable controlled this wide variation in transport behavior. Nevertheless, the intragranularlike nature of the V-J curves of the 7° bicrystal seen in Fig. 3(a) provides further evidence that some 7° grain boundaries do not restrict the supercurrent across them, while others pose a significant barrier.

V. DISCUSSION AND CONCLUSIONS

Extensive characterizations of pulsed-laser-deposited [001] tilt $YBa_2Cu_3O_{7-x}$ bicrystals have revealed several new features of the current transport across grain boundaries lying in the low to high misorientation angle range. Zero-field measurements of J_b/J_c versus θ reveal that there are two different regimes of behavior for the PLD bicrystals in this study and that the ratio J_b/J_c for the PLD bicrystals is generally larger than that found earlier for electron-beam evaporated bicrystals. From 0° to 7°, $J_b/J_c \approx 1$, with essentially no misorientation angle dependence for the samples with the highest J_b/J_c values. This result is striking and not in agreement with dislocation overlap models. It also suggests significant material-dependent preparation effects, as we now discuss.

The underlying basis for dislocation core or strain-field overlap models is discussed in Refs. 1 and 15. Assuming a symmetrical tilt boundary, the grain-boundary dislocation (GBD) spacing D, as a function of misorientation angle θ, is given by[28]

$$D = |\mathbf{b}|/[2\sin(\theta/2)], \tag{2}$$

where $|\mathbf{b}|$ is the magnitude of the GBD Burgers vector. High-resolution transmission electron micrographs of the grain boundaries in our laser-ablated films show that these Burgers vectors are of the $a[100]$ type, with magnitude 0.39 nm,[17] although evidence from studies of bulk scale bicrystals[18,19] indicates that multiple Burgers vectors can coexist in the same GB (e.g., $a/2[110], a[100], a[110]$). Within the assumptions of the overlap models, transport across low-angle GB's is primarily determined by the fractional area $[1-(D-2r_m)]$ of strongly coupled channel. Using the low-angle limit of Eq. (2) ($D \sim b/\theta$), Chisholm and Pennycook[15] predicted that the ratio of the inter- and intragrain critical current densities should linearly decline with increasing θ, following $J_b/J_c \approx 1-2r_m\theta/|\mathbf{b}|$. By assuming a crossover misorientation angle from strong-to-weak coupling at 10°, they found a large, strain-enhanced GBD radius of $r_m = 2.9|\mathbf{b}|$.

In fact, a crossover from strongly to weakly coupled behavior is expected when the channel width goes below $\sim\xi$, rather than when it goes to zero. This does not simplify the problem however, since the effective GBD core radius is so uncertain. Usually, r_m is assumed to be equal to $|\mathbf{b}|$, by estimating the size of the cation disordered region,[16] but it might be as large as the $2.9|\mathbf{b}|$ suggested in Ref. 15. From the measured H_{c2} of $YBa_2Cu_3O_{7-x}$,[29] one finds $\xi(77\,\mathrm{K}) \approx 3.5\,\mathrm{nm}$, suggesting a strong-to-weak coupling transition θ_c at $\sim 6°$ at 77 K and $\sim 8°$ at 4 K. Plotted as dashed lines in Fig. 1 are the predictions of the channel model for $r_m = 0.39$ and $1.13(2.9|\mathbf{b}|)$ nm.[1,15] The changes from long to short dashes indicate when the channels between the dislocation cores become less than a coherence length wide at 77 K. Since the coherence length decreases with temperature, channels should be smaller at 5 than at 77 K, and the ratio of J_b/J_c and the crossover angle should be larger at 5 than at 77 K. In fact, the EBE data at 5 K and our PLD data at 77 K explicitly contradict such a prediction.

We believe that the underlying reason for this variability of behavior lies in the extreme sensitivity of the GB channels to film formation conditions. There was significant scatter in the J_c values of several low-angle bicrystals with the same θ, even though all substrates of a given misorientation came from the same batch and all films were made in nominally the same way. Particular study of the films made on four 7° [001] tilt bicrystal substrates showed that the ratio $J_b/J_c(77\,\mathrm{K})$ varied from 0.3 to 0.95, indicating a strong sensitivity to small changes in growth parameters. This variability leads us to postulate that the underlying cause of the differences in the 7° [001] tilt bicrystals shown in Fig. 4 is small variations in the effective channel widths across each GB due to small differences in film growth temperature and thermal history.

The grain boundary in film Y692*s*-*b*(7°) [Fig. 4(a)] shows practically no influence of the boundary, while the two others share a distinct ''kink'' in the higher voltage parts of the characteristics that reflects dissipation within the boundary, which is quite obvious in the *V*-*J* data taken on the 10° bicrystals. We believe that the principal factor controlling the channel width is the extent of diffusion up from the substrate. Sr and Ti can diffuse into the bulk of the $YBa_2Cu_3O_{7-\delta}$ during film growth[30] thus making it very likely that there is preferential diffusion along the dislocation cores. Substitution or addition of Sr^{2+} or Ti^{4+} to the core can only increase the effective core radius and diminish the channel width, adding resistance to the boundary, thus explaining the variation in the observed properties.

To understand the underlying reasons for misorientation angle effects in low-angle boundaries, it is thus appropriate to consider the ''best,'' rather than the ''worst,'' bicrystals. As Fig. 1 shows, the data indicate two quite distinct functions for $J_b(\theta)$. Up to about 7°, there can be little or no diminution of current density, while above 7°, J_b shows the same exponential dependence on θ, which is already well known from experiments on higher angle [001] thin-film tilt bicrystals. Somewhat surprisingly, there appears to be no barrier to intergranular current flow at lower angles, and the simple linear decrease in J_b/J_c for small θ expected within the dislocation core overlap model was not observed.

One factor that may keep the J_b/J_c ratio high at low angles is that the grain-boundary dislocations can act as strong pinning centers, akin to those produced by heavy-ion irradiation. Their effective density at 7° corresponds to the vortex spacing at $\sim$20 T, setting up the possibility that the *intergranular* pinning may actually be stronger than the *intragranular* pinning in the banks on either side of the GB. A significant pinning effect of grain-boundary dislocations has recently been seen by Diaz *et al.*[31] in a 4° [001] $YBa_2Cu_3O_{7-\delta}$ thin film and by Cai *et al.*[32] in several bulk scale boundaries of higher angle.

A second, independent factor that can keep J_b high at low angles arises within the framework of the model of Kupriyanov *et al.*,[33] in which the channels are long enough and narrow enough to be unable to support vortices. Transport then takes place at the depairing current density. Since the depairing density for a full gap exceeds $10^7\,\mathrm{A/cm^2}$ at 77 K, even a large fraction of nonsuperconducting dislocation cores can still leave enough narrow channels across the GB to support the $1-3\times10^6\,\mathrm{A/cm^2}$ that is supported by flux pinning within the grains on either side of the grain boundary. However, this mechanism breaks down when the channels become so small that strong proximity effect depression of the order parameter and J_d occurs. Such a model makes it clear that the ratio J_b/J_c depends both on J_b and the intragranular critical current density, J_c at low misorientation angles. Consistent with this, we generally observe open channels up to misorientation angles of at least 20° for bulk-scale $YBa_2Cu_3O_{7-x}$ bicrystals, which have significantly lower intragranular critical current densities ($\sim 5\times10^3\,\mathrm{A/cm^2}$ at 77 K, 0 T versus $10^6\,\mathrm{A/cm^2}$ for the thin films).

A detailed model of the grain boundary which incorporates the influence of the grain-boundary dislocation structure and the strain effects that they produce has been presented recently by Gurevich and Pashitski.[34] The basic postulate is the proximity of all high-temperature superconductors to the metal-insulator transition. It is well known from electron-energy-loss measurements on Y-Ba-Cu-O grain boundaries that the boundaries tend to become hole poor as θ increases, leading to a depression of the chemical potential and an increase in the dielectric screening length at the boundary. Thus, although channels of width less than ξ, as seen in bicrystals having $\theta\sim5-10°$, may support critical currents at the depairing level, in fact the dielectric properties of the dislocation cores produce a strong depression of the channel properties. Diffusion of foreign atoms from the substrate along the dislocation cores will only exacerbate this tendency, narrowing the channels and producing a strong to weak coupling crossover at even lower angles, consistent with the behavior observed here.

To test these ideas of open channels, it is important to have an experimental test of whether or not strongly coupled channels across the grain boundary exist. To search for them, we measured the extended voltage-current density (*V*-*J*) characteristics, looking for the transition from clearly single crystal-like behavior to clearly Josephson-coupled behavior. High magnetic-field measurements of irreversibility field, $H^*(77\,\mathrm{K})$, were made to determine the closure of strongly coupled channels across the grain boundary. In the PLD films, the measured values of the intergranular H^* were

close to the intragranular values up to a misorientation angle of 10°, above which H^* became much smaller than the intragranular values.

We conclude that the measured closure of strongly coupled grain-boundary channels occurs at $10° < \theta_c \leqslant 15°$. This value of θ_c is higher than that derived from zero-field measurements. Dislocation overlap models thus need to take account of the detailed structure of the channels between the cores. Study of the extended V-J curves of several $\theta = 7°$ thin-film bicrystals indicates that one showed no evidence of weak coupling in high fields, supporting the conclusion from the zero-field data that some 7° bicrystals do not restrict the supercurrent. The implication is that weak coupling in low-angle grain boundaries ($\leqslant 7°$) of $YBa_2Cu_3O_{7-x}$ has a significant film growth and processing component. Given the present strong interest in the many types of biaxially oriented coated conductors, this issue now becomes one of practical, and not just conceptual importance.

ACKNOWLEDGMENTS

The authors wish to thank George Daniels, Bruce Davidson, and Ariane Holper for advice and assistance with the thin-film fabrication and processing, X. Y. Cai, Michael Field, and Alexander Gurevich for discussions concerning the electromagnetic properties and Susan Babcock and I Fei Tsu for conversations regarding grain-boundary microstructure. This work was supported by the NSF Materials Research Group Program (DMR-9214707), the NSF MRSEC Program (DMR-9632527), and the Electric Power Research Institute (RP8065-6).

[1] D. Dimos, P. Chaudhari, and J. Mannhart, Phys. Rev. B **41**, 4038 (1990); D. Dimos, P. Chaudhari, J. Mannhart, and F. K. LeGoues, Phys. Rev. Lett. **61**, 219 (1988).

[2] R. Gross, in *Interfaces in Superconducting Systems*, edited by S. L. Shindé and D. Rudman (Springer-Verlag, New York, 1992).

[3] T. Amrein, L. Schultz, B. Kabius, and K. Urban, Phys. Rev. B **51**, 6792 (1995).

[4] Z. G. Ivanov, P. Å. Nilsson, D. Winkler, J. A. Alarco, T. Claeson, E. A. Stepantzov, and A. Ya. Tzalenchuk, Appl. Phys. Lett. **59**, 3030 (1991).

[5] M. Kawasaki, E. Sarnelli, P. Chaudhari, A. Gupta, A. Kussmaul, J. Lacey, and W. Lee, Appl. Phys. Lett. **62**, 417 (1993); E. Sarnelli, P. Chaudhari, W. Y. Lee, and E. Esposito, *ibid.* **65**, 362 (1994).

[6] M. B. Field, X. Y. Cai, S. E. Babcock, and D. C. Larbalestier, IEEE Trans. Supercond. **3**, 1479 (1993); M. B. Field, D. C. Larbalestier, A. Parikh, and K. Salama, Physica C **280**, 221 (1997).

[7] D. A. Willén and K. Salama, Physica C **201**, 311 (1992).

[8] V. R. Todt, X. F. Zhang, D. J. Miller, M. St. Louis-Weber, and V. P. Dravid, Appl. Phys. Lett. **69**, 3746 (1996).

[9] Y. Iijima, N. Tanabe, O. Kohno, and Y. Ikeno, Appl. Phys. Lett. **60**, 769 (1992).

[10] R. P. Reade, P. Berdahl, R. E. Russo, and S. M. Garrison, Appl. Phys. Lett. **61**, 2231 (1992).

[11] S. R. Foltyn, P. Tiwari, R. C. Dye, M. Q. Le, and X. D. Wu, Appl. Phys. Lett. **63**, 1848 (1993); X. D. Wu, S. R. Foltyn, P. Arendt, J. Townsend, C. Adams, I. H. Campbell, P. Tiwari, Y. Coulter, and D. E. Peterson, *ibid.* **65**, 1961 (1994); X. D. Wu, S. R. Foltyn, P. N. Arendt, W. R. Blumenthal, I. H. Campbell, J. D. Cotton, J. Y. Coulter, W. L. Hults, M. P. Maley, H. F. Safar, and J. L. Smith, *ibid.* **67**, 2397 (1995).

[12] A. Knierim, R. Auer, J. Geerk, G. Linker, O. Meyer, H. Reiner, and R. Schneider, Appl. Phys. Lett. **70**, 661 (1997).

[13] A. Goyal, D. P. Norton, J. D. Budai, M. Paranthaman, E. D. Specht, D. M. Kroeger, D. K. Christen, Q. He, B. Saffian, F. A. List, D. F. Lee, P. M. Martin, C. E. Klabunde, E. Hartfield, and V. K. Sikka, Appl. Phys. Lett. **69**, 1795 (1996); D. P. Norton, A. Goyal, J. D. Budai, D. K. Christen, D. M. Kroeger, E. D. Specht, Q. He, B. Saffian, M. Paranthaman, C. E. Klabunde, D. F. Lee, B. C. Sales, and F. A. List, Science **274**, 755 (1996).

[14] A. Polyanskii, A. Pashitski, A. Gurevich, J. A. Parrell, M. Polak, D. C. Larbalestier, S. R. Foltyn, and P. N. Arendt (unpublished); A. E. Pashitski, A. Gurevich, A. A. Polyanski, D. C. Larbalestier, A. Goyal, E. D. Specht, D. M. Kroeger, J. A. Deluca, and J. E. Tkaczyk, Science **275**, 367 (1997); D. C. Larbalestier, *ibid.* **274**, 736 (1996).

[15] M. F. Chisholm and S. J. Pennycook, Nature (London) **351**, 47 (1991).

[16] Y. Gao, K. L. Merkle, G. Bai, H. L. M. Chang, and D. J. Lam, Ultramicroscopy **37**, 326 (1991); Physica C **174**, 1 (1991).

[17] I Fei Tsu, Ph.D. thesis, University of Wisconsin-Madison, 1996.

[18] I Fei Tsu, S. E. Babcock, and D. L. Kaiser, J. Mater. Res. **11**, 1383 (1996).

[19] Y. Zhu, J. M. Zhuo, A. R. Moodenbaugh, and M. Suenaga, Philos. Mag. A **70**, 969 (1994); S. E. Russek, D. K. Lathrop, B. H. Moeckly, R. A. Buhrman, D. H. Shin, and J. Silcox, Appl. Phys. Lett. **57**, 1155 (1990); B. H. Moeckly, D. K. Lathrop, and R. A. Buhrman, Phys. Rev. B **47**, 400 (1993).

[20] S. E. Babcock, X. Y. Cai, D. L. Kaiser, and D. C. Larbalestier, Nature (London) **347**, 167 (1990).

[21] X. Y. Cai *et al.* (unpublished).

[22] A. S. Parikh, B. Meyer, and K. Salama, Supercond. Sci. Technol. **7**, 455 (1994).

[23] N. F. Heinig, R. D. Redwing, I. F. Tsu, A. Gurevich, J. E. Nordman, S. E. Babcock, and D. C. Larbalestier, Appl. Phys. Lett. **69**, 577 (1996).

[24] R. H. Koch, V. Foglietti, W. J. Gallagher, G. Koren, A. Gupta, and M. P. A. Fisher, Phys. Rev. Lett. **63**, 1511 (1989).

[25] H. S. Edelman, J. A. Parrell, and D. C. Larbalestier, J. Appl. Phys. **81**, 2296 (1997).

[26] J. A. Parrell, D. C. Larbalestier, G. N. Riley, Jr., Q. Li, R. D. Parrella, and M. Teplitsky, Appl. Phys. Lett. **69**, 2915 (1996).

[27] Qiang Li, M. Suenaga, Qi Li, and T. Freltoft, Appl. Phys. Lett. **64**, 250 (1994).

[28] J. Weertman and J. R. Weertman, *Elementary Dislocation Theory* (Oxford University Press, New York, 1992), p. 189.

[29] U. Welp, W. K. Kwok, G. W. Crabtree, K. G. Vandervoort, and J. Z. Liu, Phys. Rev. Lett. **62**, 1908 (1989).

[30] B. W. Hussey, A. Gupta, and E. Olsson, J. Appl. Phys. **76**, 2807 (1994).

[31] A. Diaz, L. Mechin, P. Berghuis, and J. E. Evetts, Phys. Rev. Lett. **80**, 3855 (1998); Phys. Rev. B **58**, R2960 (1998).

[32] X. Y. Cai, A. Gurevich, I-Fei Tsu, D. L. Kaiser, S. E. Babcock, and D. C. Larbalestier, Phys. Rev. B **57**, 10 951 (1998).

[33] M. Yu. Kupriyanov, K. K. Likharev, and L. A. Maslova, in *Proceedings of the 14th International Conference on Low Temperature Physics*, edited by M. Krusius and M. Vuorio (North-Holland, Amsterdam, 1975), Vol. 4, p. 104.

[34] A. Gurevich and E. A. Pashitski, Phys. Rev. B **57**, 13 878 (1998); **56**, 6213 (1997).